1-1-2013

Anisotropy of crystal growth mechanisms, dielectricity, and magnetism of multiferroic Bi2FeMnO6 thin films

P Liu
University of Wollongong

Z X. Cheng
University of Wollongong, cheng@uow.edu.au

Y Du
University of Wollongong, ydu@uow.edu.au

L Y. Feng
University of Wollongong, lf997@uowmail.edu.au

H Fang
University of Wollongong

See next page for additional authors

Anisotropy of crystal growth mechanisms, dielectricity, and magnetism of multiferroic Bi2FeMnO6 thin films

Abstract

Epitaxial Bi2FeMnO6 (BFMO) thin films deposited on various Nb:SrTiO3 substrates show that the lattice parameters are very sensitive to epitaxial strains. Compressive and tensile strains are induced to the in-plane lattice constants of the (100) and (111) oriented films, respectively, while that of the (110) oriented thin film stay unstrained. The thin films also exhibit a strongly anisotropic growth habit depending on the substrate. Spiral growth, such as in the (100) BFMO film, is unique in samples prepared by pulsed laser deposition. Extrinsic dielectric constants at low frequencies are attributed to oxygen vacancies via the Maxwell-Wagner effect. All the samples show saturated hysteresis loops with very small coercive fields at 200 K, indicating the presence of weak ferromagnetism.

Keywords

crystal, growth, mechanisms, dielectricity, anisotropy, magnetism, films, multiferroic, bi2femno6, thin

Disciplines

Engineering | Physical Sciences and Mathematics

Publication Details

Liu, P., Cheng, Z. X., Du, Y., Feng, L., Fang, H., Wang, X. L. & Dou, S. X. (2013). Anisotropy of crystal growth mechanisms, dielectricity, and magnetism of multiferroic Bi2FeMnO6 thin films. Journal of Applied Physics, 113 (17), 17D904-1-17D904-3.

Authors

P Liu, Z X. Cheng, Y Du, L Y. Feng, H Fang, Xiaolin Wang, and S X. Dou

AIP | Journal of Applied Physics

Anisotropy of crystal growth mechanisms, dielectricity, and magnetism of multiferroic Bi2FeMnO6 thin films

P. Liu, Z. X. Cheng, Y. Du, L. Y. Feng, H. Fang et al.

Citation: J. Appl. Phys. 113, 17D904 (2013); doi: 10.1063/1.4794724
View online: http://dx.doi.org/10.1063/1.4794724
View Table of Contents: http://jap.aip.org/resource/1/JAPIAU/v113/i17
Published by the American Institute of Physics.

JOURNAL OF APPLIED PHYSICS **113**, 17D904 (2013)

Anisotropy of crystal growth mechanisms, dielectricity, and magnetism of multiferroic Bi_2FeMnO_6 thin films

P. Liu, Z. X. Cheng,[a] Y. Du, L. Y. Feng, H. Fang, X. L. Wang,[a] and S. X. Dou
Institute for Superconducting and Electronic Materials, University of Wollongong, Squires Way, North Wollongong, New South Wales 2500, Australia

(Presented 18 January 2013; received 29 October 2012; accepted 28 November 2012; published online 11 March 2013)

Epitaxial Bi_2FeMnO_6 (BFMO) thin films deposited on various Nb:$SrTiO_3$ substrates show that the lattice parameters are very sensitive to epitaxial strains. Compressive and tensile strains are induced to the in-plane lattice constants of the (100) and (111) oriented films, respectively, while that of the (110) oriented thin film stay unstrained. The thin films also exhibit a strongly anisotropic growth habit depending on the substrate. Spiral growth, such as in the (100) BFMO film, is unique in samples prepared by pulsed laser deposition. Extrinsic dielectric constants at low frequencies are attributed to oxygen vacancies via the Maxwell-Wagner effect. All the samples show saturated hysteresis loops with very small coercive fields at 200 K, indicating the presence of weak ferromagnetism. © *2013 American Institute of Physics*. [http://dx.doi.org/10.1063/1.4794724]

Multiferroic materials exhibiting coupling between magnetic and ferroelectric order parameters have attracted much attention from both the application and the fundamental physics points of view.[1,2] $BiFeO_3$ and $BiMnO_3$ are two promising multiferroics that have been extensively studied.[3–6] $BiFeO_3$, exhibiting ferroelectricity (FE) below 1103 K and antiferromagnetism below 640 K, is the only room-temperature single phase multiferroic material.[3] It has a spiral cycloid antiferromagnetic structure with a wavelength of 62 nm along the $[1\ 1\ 0]_h$ axis.[4] $BiMnO_3$ is of significance to simultaneously possess ferromagnetic (below 105 K) and ferroelectric (below 450 K) orders.[5,6] In terms of exploring more room-temperature ferroelectric ferromagnetic materials, which are critical for next-generation spintronic devices, the double-perovskite oxides $Bi_2BB'O_6$ (B, B′ = 3d transition-metal ion) were predicted to be good candidates by first-principles calculations.[7] $6s^2$ lone pair electrons of the Bi^{3+} cation induce ferroelectric polarization, whilst the superexchange interactions between B and B′ lead to ferromagnetism through B–O–B′–O–B ordering.[8] Among these materials, Bi_2NiMnO_6 and Bi_2FeCrO_6 have been widely investigated.[9,10] By contrast, little research work has been focused on metastable Bi_2FeMnO_6 (BFMO) due to phase instability and the high volatility of bismuth. BFMO, possessing the rhombohedral R3*c* symmetry, was reported to exhibit magnetic transitions at 150 K, 260 K, and 440 K, respectively, corresponding to Fe–O–Mn, Mn–O–Mn, and Fe–O–Fe orderings.[11] The FE of BFMO was confirmed by the presence of piezoelectric hysteresis.[12] Neutron diffraction of BFMO thin film deposited on (001) $SrTiO_3$ (STO) substrate suggested the absence of the cycloid AFM structure and a random distribution of Mn and Fe ions over B-sites.[13] The strained BFMO thin film grown on (001) STO substrate also shows strong enhancement of the magnetization and the magnetic transition temperature.[14] Thus, it is highly important to further examine the strain effects of substrates on the epitaxial growth, microstructure, and dielectric properties of BFMO thin films. In the present work, epitaxial BFMO thin films were successfully deposited on different Nb doped $SrTiO_3$ substrates (NSTO). Anisotropy in topographic, magnetic, and dielectric properties was clearly observed. We found that the substrate orientation dominates crystal growth behaviour of our samples. In particular, BFMO thin film deposited on NSTO (100) substrate shows a morphology of spiral growth that is attributed to screw dislocation (SD) defects.

BFMO thin films were grown from a $Bi_{2.1}FeMnO_6$ ceramic target on conductive (100), (110), and (111) NSTO substrates by pulsed laser deposition (PLD). The third harmonic generation of a 355 nm Nd:YAG laser was used with a laser energy density of 3.8 J/cm^2 and a laser pulse rate of 10 Hz. The deposition conditions have been optimized to be 700 °C, 550 mTorr dynamic oxygen, and 1 h growth. The samples were characterized by X-ray diffraction (XRD), field emission scanning electron microscopy (FESEM) equipped with energy dispersive spectroscopy (EDS), and atomic force microscopy (AFM). The dielectric properties of the thin films, with gold dots as top electrodes, were measured from 40 Hz to 4 MHz using an HP 4194A Impedance Analyzer. The magnetic properties were examined via a physical properties measurement system (PPMS, Quantum Design).

The XRD patterns in Fig. 1 show that the as-prepared thin films feature quality single phase epitaxial growth, in agreement with a previous report.[15] The thin films were epitaxially crystallized in the pseudo-cubic structure along the $(100)_c$, $(110)_c$, and $(111)_c$ directions on (100), (110), and (111) NSTO substrates, respectively. The corresponding out-of-plane pseudo-cubic lattice parameters are 3.986, 3.961, and 3.94 Å, respectively. The lattice parameter a_c of the pseudo-cubic $BiFeO_3$ cell was previously reported to be

[a]Authors to whom correspondence should be addressed. Electronic addresses: cheng@uow.edu.au and xiaolin@uow.edu.au.

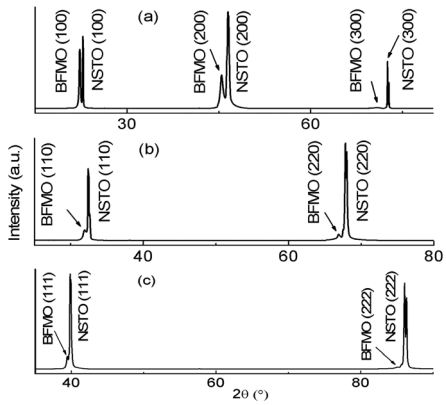

FIG. 1. Out-of-plane XRD patterns of the BFMO thin films.

3.963 Å, from which our measured lattice parameters obviously deviate as a result of manganese doping and lattice mismatch with the substrate.[16] In comparison with pseudo-cubic $BiFeO_3$, the out-of-plane lattice parameter of epitaxial BFMO thin film increases on (100) NSTO, remains constant on (110) NSTO, but decreases on (111) NSTO. Accordingly, compressive and tensile strains are induced to the in-plane lattice constants of the (100) and (111) oriented films, respectively, while that of the (110) oriented thin film stay unstrained. The thin films were determined to be around 90 nm thick.

The AFM surface topographies of the thin films are presented in Fig. 2. The surface morphologies are quite different from each other as a result of epitaxy along various directions. The BFMO (110) thin film shows stripe growth in the (110) plane, with root-mean-square (RMS) surface roughness of 10.0 nm. Widths of stripe grains vary from 40 nm to 160 nm. More interesting features were observed in the BFMO (111) sample, namely, the coexistence between small rough grains and large square grains. The RMS surface roughness is around 13.8 nm. Small round grains with sizes from 50 nm to

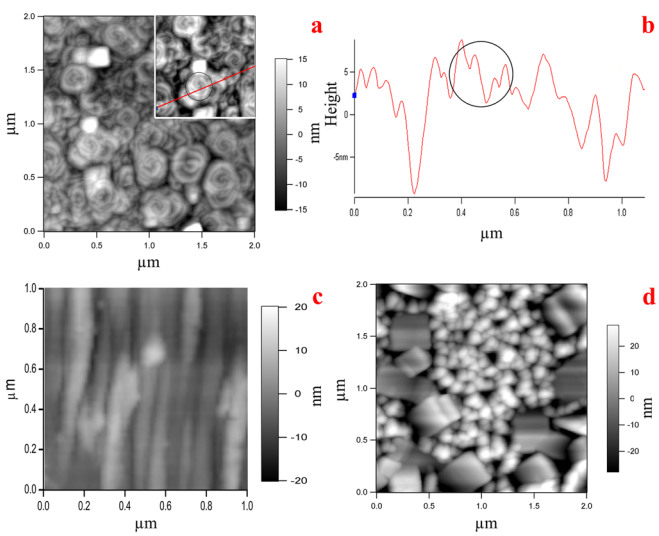

FIG. 2. AFM images of the (a) (100), (c) (110), and (d) (111) oriented BFMO thin films. The inset of (a) shows a quality image of a 1 μm^2 area, and the height variations on the red line are presented in (b).

200 nm indicate oriented growth along the pseudo-cubic [111] direction. Large square grains mounted among the round grains have variable sizes from 200 nm to 500 nm.

It is remarkable that the BFMO (100) thin film has a smooth surface with a spiral crystal growth pattern along the [100] direction. The RMS surface roughness is around 4.5 nm. The circular spirals are isotropic, with step spacing of about 35 nm. Spiral step-lines are densely distributed in the thin film, in which spirals have sizes ranging from 120 nm to 330 nm. In most spiral units, two steps turn around their own point of emergence in the same direction, forming co-rotating spiral ridges.[17] Such spiral growth observed in the thin film is due to formation of SDs in the process of deposition. A SD is a kind of line defect required to be normal to the surface. When a SD intersects the surface, a depression in the surface will be generated by the dislocation line's tension and provides a preferred site for atoms to bond, greatly raising the growth rate. A step arises from the intersection point and stays immobile at the SD. Throughout the deposition process, the step winds up around the SD to form a spiral ridge.[18] High deposition temperature is responsible for the isotropic spirals, because the spirals should become anisotropic to reflect the crystal symmetry at low temperatures.[18] The large density of spirals with no more than two turns indicates that the SDs are densely concentrated over the whole thin film. Otherwise, longer distances between SDs would allow larger spirals with more turns to come into being. In conventional spiral growth from an aqueous solution or flux, terraces are constructed from atomically flat layers to keep pace with the continuous advancement of steps.[19] The centres of spirals are raised during growth, leading to a hillock surface structure. The features of our sample, however, have a few differences from those of conventional spiral growth, which can be seen in Fig. 2(b). This sample shows the slowest growth at the spiral centre, and faster growth as the distance from the spiral centre increases. It is evident that terrace layer growth is absent from the BFMO (100) thin film. The differences can be understood by comparing the dissimilarities of the crystalline conditions. In conventional spiral growth, aqueous solutions allow atoms to be uniformly absorbed around SDs after effectively moving, and they then go on to create atomically flat terraces. For PLD, atoms contained in the plasma are locally confined to the area where they reach the substrate surface. Atoms tend to simultaneously crystallize around the closest defects to form spiral ridges.

The FESEM surface morphologies shown in Fig. 3 are consistent with the observations from AFM images. Spiral growth was doubly confirmed in the BFMO (100) thin film. Stripe structures were also supported by the SEM surface morphology of the BFMO (110) sample. More exact surface details for the BFMO (111) film were obtained from the FESEM images. Small grains actually exist in the shape of pyramids, suggesting the [111] direction of epitaxial growth. Large grains are linked to each other at an angle of 120°, forming hexagons. It is important to check for composition differences between large and small grains in such a case. The EDS results show that their compositions are identical, supporting the absence of any impurity peaks in the XRD

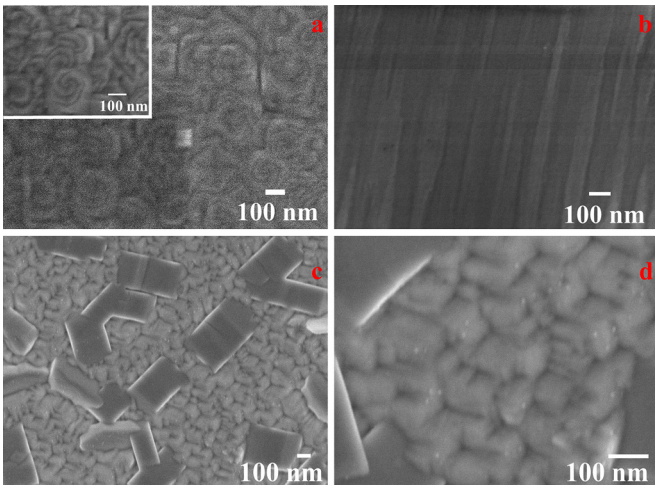

FIG. 3. FESEM images of the (a) (100), (b) (110), and (c) (111) thin films. (d) and the inset of (a) show magnified images of the BFMO (111) and (100) thin films, respectively.

patterns. Thus, large hexagons are caused by disequilibrium crystallization due to lattice mismatch between the thick overlay and the substrate.

The frequency-dependent relative dielectric constant and dielectric loss of the thin films are shown in Fig. 4. The relative dielectric constants decrease monotonically with increasing frequency, but only slightly at frequencies higher than 30 kHz. The relative dielectric constant values at 1 MHz are 130, 56, and 36 for BFMO (100), BFMO (111), and BFMO (110), respectively. Dielectric losses also show similar decreasing trends with increasing frequency, except that they display peaks below 200 kHz. The corresponding dielectric losses at 1 MHz are 0.34, 0.38, and 0.20. Our dielectric data on the BFMO thin films are in good agreement with the previous reports on BFMO ceramics.[20,21] The reductions in both the dielectric constant and the dielectric loss with increasing frequency suggest that the high values of the dielectric constant and dielectric loss at low frequencies are not intrinsic to the thin films, but are rather associated with conductive properties.[20] As shown in Fig. 4, an dielectric relaxation process is observed in the dielectric loss measurements below 200 kHz, but it is absent from the dielectric constant data over that range of frequency. This observation further demonstrates that extrinsic dielectric values at low frequencies could be attributed to the Maxwell-Wagner effect, namely, interfacial polarization generated by quasi-mobility of locally uncompensated space charges.[22]

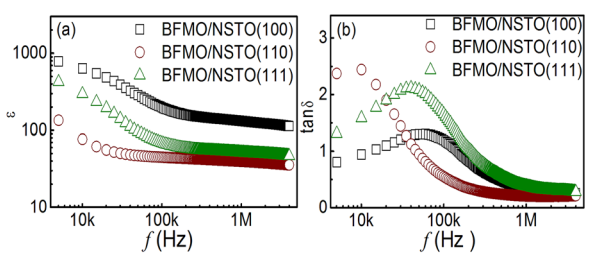

FIG. 4. Frequency dependence of the relative dielectric constant and loss at room temperature.

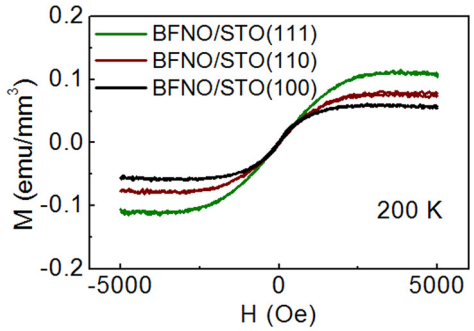

FIG. 5. In-plane isothermal magnetization curves of the samples at 200 K.

Fig. 5 presents the in-plane isothermal magnetization curves of the samples at 200 K. All the samples show saturated hysteresis loops with very small coercive fields, indicating the presence of weak ferromagnetism. The magnetizations at 5000 Oe are 0.057 emu/mm^3, 0.078 emu/mm^3, and 0.109 emu/mm^3, corresponding to the BFMO (100), BFMO (110), and BFMO (111) thin films, respectively. Thus, magnetic anisotropy is induced by substrate strains via the magneto-elastic effect. Our observations are similar to those in other reports, but with relatively larger magnetizations.[23]

In conclusion, epitaxial BFMO thin films of single phase were successfully prepared by the PLD method on (100), (110), and (111) NSTO substrates, respectively. Strain effects give rise to completely different surface morphology features. In particular, the spiral growth observed in the BFMO (100) thin film is due to formation of SDs in the process of deposition. All the samples show weak ferromagnetism at 200 K indicated by saturated hysteresis loops with very small coercive fields. The extrinsic dielectric values at low frequencies could be attributed to the Maxwell-Wagner effect.

Author Z. X. Cheng thanks the Australian Research Council for support through a Future Fellowship (FT 0990287).

[1]W. Eerenstein, N. D. Mathur, and J. F. Scott, Nature **442**, 759 (2006).
[2]N. A. Spaldin and M. Fiebig, Science **309**, 391 (2005).
[3]Z. X. Cheng *et al.*, Phys. Rev. B **77**, 092101 (2008).
[4]F. Zavaliche *et al.*, Appl. Phys. Lett. **87**, 182912 (2005).
[5]F. Sugawara *et al.*, J. Phys. Soc. Jpn. **20**, 1529 (1965).
[6]A. F. M. dos Santos *et al.*, Appl. Phys. Lett. **84**, 91 (2004).
[7]Y. Uratani, T. Shishidou, F. Ishii, and T. Oguchi, Physica B **383**, 9 (2006).
[8]R. I. Dass and J. B. Goodenough, Phys. Rev. B **67**, 014401 (2003).
[9]R. Nechache *et al.*, Appl. Phys. Lett. **89**, 102902 (2006).
[10]M. N. Iliev, P. Padhan, and A. Gupta, Phys. Rev. B **77**, 172303 (2008).
[11]Y. Du *et al.*, Appl. Phys. Lett. **97**, 122502 (2010).
[12]S. H. Lee *et al.*, Physica B **383**, 31 (2006).
[13]D. L. Cortie *et al.*, Appl. Phys. Lett. **101**, 172404 (2012).
[14]E. M. Choi *et al.*, Appl. Phys. Lett. **98**, 012509 (2011).
[15]L. Bi *et al.*, Phys. Rev. B **78**, 104106 (2008).
[16]V. V. Lazenka *et al.*, J. Phys. D: Appl. Phys. **45**, 125002 (2012).
[17]P. Smereka, Physica D **138**, 282 (2000).
[18]W. K. Burton *et al.*, Philos. Trans. R. Soc. London **243**, 299 (1951).
[19]X. L. Wang *et al.*, Phys. Rev. B **55**, R3402 (1997).
[20]A. Ianculescu *et al.*, J. Alloys Compd. **504**, 420 (2010).
[21]D. K. Pradhan *et al.*, J. Appl. Phys. **106**, 024102 (2009).
[22]A. K. Jonscher, J. Mater. Sci. **16**, 2037 (1981).
[23]J. Miao *et al.*, Appl. Phys. Lett. **99**, 062905 (2011).